EMBEDDED MULTIPLE DESCRIPTION SCALAR QUANTIZERS AND WAVELET-BASED QUADTREE CODING FOR PROGRESSIVE IMAGE TRANSMISSION OVER UNRELIABLE CHANNELS

*A. I. Gavrilescu, A. Munteanu, J. Cornelis, P. Schelkens

Vrije Universiteit Brussel
Department of Electronics and Information Processing (ETRO)
* Email: aigavril@etro.vub.ac.be

ABSTRACT

In this paper, we present a new Multiple Description Coding (MDC) system that enables the progressive transmission of images over unreliable channels with variable bandwidth. The proposed system employs a new type of quantizers, called Embedded Multiple Description Scalar Quantizers (EMDSQ). The system relies on wavelet-based QuadTree (QT) coding of the significance maps to encode the quantizers' output, and is referred to as Multiple Description-QT (MD-QT) coding. The EMDSQ enables the MD-QT coder to provide bit-streams that meet the desired features consisting of a high redundancy level, fine-grain rate adaptation and progressive transmission of each description. Experimental results show that the proposed MD-QT system based on EMDSQ yields better rate-distortion performance in comparison to MD-QT employing the embedded Multiple Description Uniform Scalar Quantizers (MDUSQ) previously proposed in the literature.

1. INTRODUCTION

Communication systems based on diversity techniques have become an attractive solution for robust transmission over error-prone bandwidth-limited channels. Multiple Description Coding (MDC) addresses the problem of coding a source in order to be transmitted over a communication network with diversity, and, at the decoder level, it allows for extracting meaningful information from a subset of the bit-stream.

Previous research focused on finding the optimal achievable rates-distortion regions [1]. Lately, practical compression systems that rely on quantization techniques, as proposed in [2], [3], were designed in order to meet those theoretical boundaries. The design of multiple description scalar quantizers (MDSQ) was pioneered in [2], under the assumption of fixed-length codes and fixed codebook sizes. Significant improvements are reported in [3] in which the quantizers' design is made under a given entropy-constraint, and not on a given codebook size.

The communication robustness over unreliable channels provided by the MDC system is strongly correlated with the delivery of highly error-resilient bit-streams, a feature achievable with a corresponding high level of redundancy. Furthermore, for bandwidth-varying channels, it is desirable to transmit fine-grain scalable bit-streams. Such a system is described in [4] where the progressive MDC algorithm is based on multiple description uniform scalar quantizers (MDUSQ). For a high level of redundancy and for low bit-rates, the approach of [4] outperforms the embedded MDC algorithm of [5] based on the polyphase transform. In the same context, we proposed in [6], [7] a new type of embedded multiple description scalar quantizer (EMDSQ), providing a fine-grain refinable representation of the input data and targeting a high level of redundancy. The embedded quantizer design follows the constraint of constructing double-deadzone central quantizers for each quantization level.

In this paper we propose a new wavelet-based MDC system that employs the EMDSQ and a customized version of the QuadTree (QT) coding of the significance maps algorithm of [8]. The system will be referred to as Multiple Description-QT (MD-QT) coding. The EMDSQ, by their features, allow the MD-QT coder to provide bit-streams that meet the desired features consisting of a high redundancy level, fine-grain rate adaptation and progressive transmission of each description. Moreover, the generalized form of EMDSQ targeting an arbitrary number of channels offers the possibility of designing realistic coders for practical multi-channel communication systems. Such systems reconstruct the central channel by using techniques such as synchronization markers to isolate the undamaged data from a partially damaged received side channel. In this context, for an erasure channel model with burst errors, progressive transmission is providing quality scalability for the central-channel reconstruction.

The MDUSQ of [4] and our EMDSQ [6], [7] are incorporated in the proposed MD-QT coding scheme. The rate-distortion performances of both MDC systems are compared when applied on a common dataset. The results demonstrate that the MDC system based on EMDSQ achieves systematically better rate-distortion performance on a broad range of bit-rates.

The paper is structured as follows. In Section 2 the EMDSQ generalized form for *M*-channels is introduced. The MD-QT coding system is described in Section 3. In Section 4 comparative coding results are provided, and finally, Section 5 draws the conclusions of our work.

2. EMBEDDED MULTIPLE DESCRIPTION SCALAR QUANTIZERS

Quantization methods based on embedded scalar quantizers were previously proposed in the literature – see for e.g. [9]. In embedded quantization, the partition cells at higher quantization rates are embedded in the partition cells of lower-rate quantizers. For the *M*-channels embedded multiple description scalar quantizers we denote the set of embedded side-quantizers as $Q_S^{m,0}$, $Q_S^{m,1}$,…, $Q_S^{m,P}$ with $m = 1..M$, and the set of embedded central-quantizers as Q_C^0, Q_C^1, …, Q_C^P, where:

$$Q_C^{p-1}(q_k^1, q_k^2, ..., q_k^M) = Q_S^{1,p-1}(q_k^1) \cap Q_S^{2,p-1}(q_k^2) \cap ... \cap Q_S^{M,p-1}(q_k^M)$$

for any quantization level p, $0 \le p \le P$. The partition cells of any quantizer $Q_S^{m,p}$ and Q_C^p are embedded in the partition cells of the quantizers $Q_S^{m,P}$, $Q_S^{m,P-1}$,…, $Q_S^{m,p+1}$ and Q_C^P, Q_C^{P-1},…, Q_C^{p+1} respectively.

For *M*-channels, the analytical expression of the EMDSQ proposed in [6], [7] is defined as follows:

$$Q_S^{m,p}(x) = \begin{cases} Q_A^{m,p}(x) & x \in \left[-A_{Sup}^{m,p}, -A_{Inf}^{m,p}\right) \cup \left[A_{Inf}^{m,p}, A_{Sup}^{m,p}\right) \\ Q_B^{m,p}(x) & x \in \left[-B_{Sup}^{m,p}, -B_{Inf}^{m,p}\right) \cup \left[B_{Inf}^{m,p}, B_{Sup}^{m,p}\right) \end{cases}, \quad (1)$$

with

$$Q_A^{m,p}(x) = sign(x)\left\lfloor \frac{|x|}{mM^p\Delta} - \frac{M+1-2m}{m}\left(k + p\%2\right)\right\rfloor, \quad (2)$$

$$Q_B^{m,p}(x) = sign(x)\left\lfloor \frac{|x|}{(M+1-m)M^p\Delta} + \frac{M+1-2m}{M+1-m}\left(k+1-p\%2\right)\right\rfloor. \quad (3)$$

The boundary points are defined as follows:

$A_{Sup}^{m,p} = \Delta \cdot M^p((M+1)k + m + (M+1-m)(p\%2))$,

$A_{Inf}^{m,p} = \Delta \cdot M^p((M+1)k + (M+1-m)(p\%2))$,

$B_{Sup}^{m,p} = \Delta \cdot M^p((M+1)k + M + 1 - m(p\%2))$,

$B_{Inf}^{m,p} = \Delta \cdot M^p((M+1)k + m - m(p\%2))$,

where $\lfloor a \rfloor$ denotes the integer part of a, $\Delta > 0$ is the cell size for Q_C^0, and $p\%2 = p - 2\cdot\lfloor p/2 \rfloor$. The index $k \in \mathbb{Z}_+$ determines the width of the quantizer granular region and m, $1 \le m \le M$ denotes the channel index.

From the expressions for $A_{Sup}^{m,p}$, $B_{Sup}^{m,p}$, $A_{Inf}^{m,p}$, $B_{Inf}^{m,p}$ given above, one notices that the cell size $\Delta^{(p)}$ for the side quantizer $Q_S^{m,p}$ at level p and index m depends on the number of channels M by $\Delta^{(p)} = M^p\Delta^{(0)}$, where $\Delta^{(0)}$ is the cell size for the highest-rate side-quantizer $Q_S^{m,0}$, and $\Delta^{(0)} = m\Delta$ or $\Delta^{(0)} = (M+1-m)\Delta$.

A noticeable characteristic of the EMDSQ is that the side-quantizers $Q_S^{m,p}$ are non-uniform embedded quantizers. Thus for any p, $1 \le p \le P$ the partition cells are divided into a variable number of sub-partition cells.

The example depicted in Fig. 1 illustrates an instantiation of the four-channel EMDSQ. In view of simplification, we consider only two quantization levels $p = 0,1$. Notice that the partitions of the side-quantizers $Q_S^{m,0}$, $1 \le m \le 4$ are embedded respectively in the partitions of the side quantizers $Q_S^{m,1}$. Moreover, we notice that the side-quantizers $Q_S^{m,p}$ are indeed non-uniform embedded quantizers: for instance, the cell $S_{+,1}^{2,1}$ of the second-channel embedded quantizer $Q_S^{2,1}$ is divided into the three partitions $S_{+,1,0}^{2,0}$, $S_{+,1,1}^{2,0}$ and $S_{+,1,2}^{2,0}$ of the higher-rate quantizer $Q_S^{2,0}$. On the contrary, the deadzone $S_0^{2,1}$ is divided into nine partitions $S_{0,0}^{2,0}$, $S_{\pm,0,1}^{2,0}$, $S_{\pm,0,2}^{2,0}$, $S_{\pm,0,3}^{2,0}$, and $S_{\pm,0,4}^{2,0}$ respectively. Notice that the central quantizer Q_C^p is a double deadzone embedded quantizer with cell-size $\Delta_C^{(p)} = 4^p\Delta_C^{(0)}$, where $\Delta_C^{(0)} = \Delta$ is the cell-size of Q_C^0.

A uniform entropy-coded scalar quantizer is optimal for high rates, and nearly optimal for lower rates [9]. Furthermore, for input data with symmetric probability density function (PDF), the rate-distortion behavior at low rates can be improved by widening the partition cell located around zero, that is, by using deadzone uniform scalar quantizers [9]. It can be noticed that the central quantizer in the EMDSQ [6], [7] is indeed a double-deadzone embedded quantizer. Hence, it shows the abovementioned characteristics.

3. CODING SCHEME

In this section, we illustrate the use of the EMDSQ into a wavelet-based coding scheme, for the particular case of $M = 2$. The proposed MD-QT coding system encodes the quantizers' output by using a customized version of the wavelet-based QT coding of the significance maps algorithm described in [8].

3.1 Significance map coding

We denote by T^p the significance threshold from the coding step corresponding to the quantization level p, $0 \le p \le P$. Denote by $\mathbf{k} = (k_1, k_2)$ the spatial location, where k_1 and k_2 stand for the row and column index, respectively. Denote by $Q(\mathbf{k}, \mathbf{v})$ a quadrant with top-left coordinates $\mathbf{k} = (k_1, k_2)$ and size $\mathbf{v} = (v_1, v_2)$, where v_1 and v_2 represent the quadrant width and height respectively. In view of simplification we assume identical power-of-two quadrant dimensions v_1 and v_2, i.e. $v_1 = v_2 = 2^J$ for some J. The corresponding quadrant delimiting binary elements in the significance map p is denoted by $Q_b^p(\mathbf{k}, \mathbf{v})$.

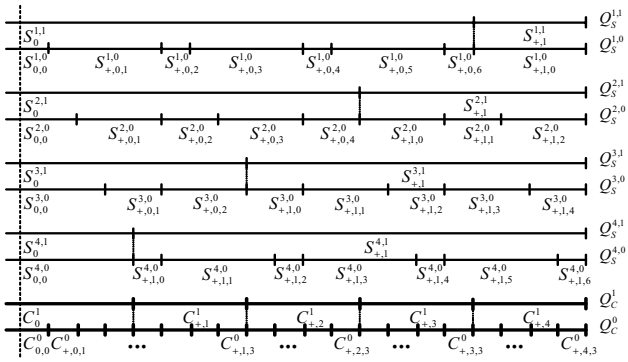

Fig. 1. Four-channel EMDSQ. The side quantizers are $Q_S^{m,p}$, with $m = 1...4$, $p = 0,1$. The central quantizer is Q_C^p. The negative side is a mirrored version of the positive side shown above.

The wavelet image $\mathbf{W} = Q(\mathbf{0}, \mathbf{V})$ is a matrix of $V_1 \times V_2$ elements, with $\mathbf{0} = (0,0)$, $\mathbf{V} = (V_1, V_2)$. For any wavelet coefficient, its absolute value and sign are denoted as $w(\mathbf{l})$ and $s(\mathbf{l})$ respectively, where $\mathbf{l} = (l_1, l_2)$ with $0 \le l_1 \le V_1$ and $0 \le l_2 \le V_2$.

The significance of the wavelet coefficients from any $Q(\mathbf{k}, \mathbf{v}) \in \mathbf{W}$, $\mathbf{v} \ne (1,1)$ with respect to the applied threshold T^p is recorded in $Q_b^p(\mathbf{k}, \mathbf{v})$ and is determined via the operator σ^p:

$$\sigma^p(Q(\mathbf{k}, \mathbf{v}))\Big|_{\mathbf{v}\ne(1,1)} = \begin{cases} 1 & if\ \exists w(\mathbf{l}) \in Q(\mathbf{k}, \mathbf{v}),\ w(\mathbf{l}) \ge T^p \\ 0 & if\ \forall w(\mathbf{l}) \in Q(\mathbf{k}, \mathbf{v}),\ w(\mathbf{l}) < T^p \end{cases} \quad (4)$$

Notice that the significance operator σ^p determines the significance of a quadrant but not the significance of a coefficient. For an individual wavelet coefficient we no longer apply the significant operator σ^p, and instead, we utilize the quantizer index allocation operator, which we denote by $\delta(w(\mathbf{l}))$.

The EMDSQ by their structure present the particularity that different partition cells at quantization level p are divided into different numbers of partition cells at the quantization level $p-1$ as shown in section 2. Thus, we deduce that in order to perform the index allocation, the wavelet coefficients have to be compared against the values of the partitions' boundary points at a certain quantization level p. Consider that an arbitrary partition cell at level p will be divided into N partition cells at level $p-1$. The index allocation operator δ determines the codeword associated to each quantized coefficient as follows:

$$\delta(w(\mathbf{l})) = \begin{cases} S_N & if\ T_{\delta,N-1} \le w(\mathbf{l}) < T_{\delta,N} \\ \dots & \\ S_2 & if\ T_{\delta,1} \le w(\mathbf{l}) < T_{\delta,2} \\ S_1 & if\ T_{\delta,0} \le w(\mathbf{l}) < T_{\delta,1} \end{cases} \quad (5)$$

where the boundary points are denoted as $T_{\delta,n}$, with $0 \le n \le N$ and $T_{\delta,0} < T_{\delta,1} < \dots < T_{\delta,N}$. The manner in which the threshold T^p and boundary points $T_{\delta,n}$ are computed will be described further under section 3.2.

For the first quadtree-partitioning pass [8], the significance of the wavelet image $\mathbf{W}$ is tested with respect to the threshold T^P. If $\sigma^P(\mathbf{W}) = 1$, the significance map $Q_b^P(\mathbf{0}, \mathbf{V})$ of the wavelet image $\mathbf{W}$ is split into four quadrants $Q_b^P(\mathbf{k}_i, \mathbf{V}/2)$, $1 \le i \le 4$, each having half the original parent size, with $\mathbf{k}_i$ indicating the origin of each quadrant. The descendent significant quadrants are then further divided until the leaf

nodes (i.e. wavelet coefficients) are isolated. For the leaf nodes, the symbols S_n ($0 < n \le N$) are allocated by applying the index allocation operator $\delta(w(\mathbf{l}))$. Thus, the significance pass records the positions $\mathbf{l}$ of all the leaf nodes newly identified as significant, using a recursive tree structure of quadrants (or a quad-tree structure).

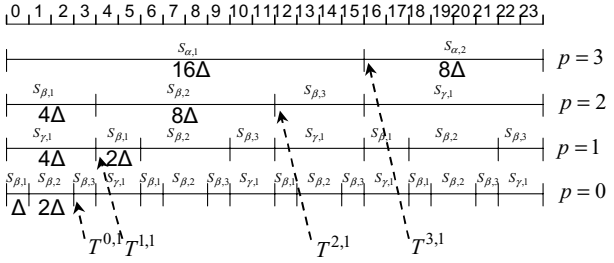

Fig. 2. Four-level representation of $Q_S^{1,P}$ for two-channel EMDSQ for an example with granular region ranging from 0 to 23. The significance map coding is performed with respect to the set of thresholds $T^{P,1}$ with the rate of decay given by (7).

Once the positions and the corresponding symbols of the significant leaf nodes are encoded during the significance pass, p is set to $P-1$. Next, the significance pass is restarted to update the entire quad-tree structure by identifying the new significant leaf nodes. During this stage, only the significance of the previously non-significant nodes and quadrants, i.e. those for which $\delta(w(\mathbf{l})) = S_1$ and $\sigma^{p+1}(Q(\mathbf{k},\mathbf{v})) = 0$ respectively, is encoded, and the significant ones are ignored since the decoder has already received this information. Subsequently, the corresponding refinement pass is activated for the significant leaf nodes. The refinement pass is performed with respect to the corresponding refinement threshold $T_r^{p,m}$. The described procedure is repeated, until the complete wavelet image is encoded, i.e. $p = 0$, or until the target bit-rate is met.

3.2 Coding algorithm

In this section, we illustrate the manner in which the significance thresholds, refinement thresholds and boundary points are computed, in the particular case of $M = 2$.

As explained before, the coding passes performed by the proposed MD-QT coding system are the significance pass, employing the significance thresholds $T^{p,m}$, $0 \le p \le P$ followed by the refinement pass, utilizing the refinement thresholds $T_r^{p,m}$, with m, $1 \le m \le 2$ denoting the channel index. For the lowest quantization rate P, the starting thresholds corresponding to each channel are $T^{P,1} = 2T$ and $T^{P,2} = T$ respectively. Since it is not desirable that the quantizer is characterized by an overload region, the T value is related to the highest absolute magnitude $w_{\max}$ of the wavelet coefficients as:

$$T = 2^{\lfloor \log_2(w_{\max}/3) \rfloor + 1} \tag{6}$$

Hence, the maximum number of quantization levels is $P = \lfloor \log_2(w_{\max}/3) \rfloor + 1$. In general, excepting the lowest quantization rate P, the significance thresholds used for each channel m, $1 \le m \le 2$ are given by:

$$T^{P-x,m} = \frac{T_m}{4^{\lfloor (x+1+(m+1)\%2)/2 \rfloor}} 3^{((x+m-1)\%2)} \tag{7}$$

with $P - x = p$, and $x \ge 1$. The values T_m are of the form $T_1 = 2T$ and $T_2 = 4T$ respectively.

Fig. 2 depicts the first channel EMDSQ with granular region ranging from 0 to 24. For the two-channel EMDSQ case, excepting the highest quantization rate P, the description of the quantizers reveals that half of the partition cells at level p are divided into three partition cells at level $p-1$, while the other half are not divided at all. Thus, we consider three index allocation operators. In the case $p = P$, we use the index allocation operator $\alpha(w(\mathbf{l}))$ to assign for the leaf-nodes in the quadtree the symbols $S_{\alpha,1}$ and $S_{\alpha,2}$ as follows:

$$\alpha(w(\mathbf{l})) = \begin{cases} S_{\alpha,2} & T_{\alpha,1}^{P,m} \le w(\mathbf{l}) < T_{\alpha,2}^{P,m} \\ S_{\alpha,1} & 0 \le w(\mathbf{l}) < T_{\alpha,1}^{P,m} \end{cases} \tag{8}$$

where $T_{\alpha,1}^{P,m} = T^{P,m}$ and $T_{\alpha,2}^{P,m} = 3T$.

In the case $p < P$ two operators $\beta(w(\mathbf{l}))$ and $\gamma(w(\mathbf{l}))$ are considered, one for each of the two partition types. For the partitions cells that are divided in three, the index allocation operator $\beta(w(\mathbf{l}))$ is expressed as:

$$\beta(w(\mathbf{l})) = \begin{cases} S_{\beta,3} & T_{\beta,2}^{p,m} \le w(\mathbf{l}) < T_{\beta,3}^{p,m} \\ S_{\beta,2} & T_{\beta,1}^{p,m} \le w(\mathbf{l}) < T_{\beta,2}^{p,m} \\ S_{\beta,1} & T_{\beta,0}^{p,m} \le w(\mathbf{l}) < T_{\beta,1}^{p,m} \end{cases} \tag{9}$$

where the relations between the corresponding partition boundary points are $T_{\beta,1}^{p,m} = T_{\beta,0}^{p,m} + \Delta_C^{(p)}$, $T_{\beta,2}^{p,m} = T_{\beta,0}^{p,m} + 3 \cdot \Delta_C^{(p)}$ and $T_{\beta,3}^{p,m} = T_{\beta,0}^{p,m} + 4 \cdot \Delta_C^{(p)}$, where $T_{\beta,0}^{P-x,m} = ((x+m)\%2)2\Delta_C^{(P-x)}$, $x \ge 1$.

Apart from this, for the remaining half of the partition cells that are not divided we assign through the index allocation operator $\gamma(w(\mathbf{l}))$ only one symbol $S_{\gamma,1}$ as follows:

$$\gamma(w(\mathbf{l})) = S_{\gamma,1} \text{ for } T_{\gamma,0}^{p,m} \le w(\mathbf{l}) < T_{\gamma,1}^{p,m} \tag{10}$$

The relation between the corresponding partition boundary points is $T_{\gamma,1}^{p,m} = T_{\gamma,0}^{p,m} + 2\Delta_C^{(p)}$, where $T_{\gamma,0}^{P-x,m} = ((x+m+1)\%2)4\Delta_C^{(P-x)}$

The purpose of the refinement pass is to perform the index allocation for coefficients that have already been coded as significant at the previous significance passes. The index allocation is performed with respect to the new updated values of the boundary points. In order to apply the index allocation, the coefficient that must be refined has to be rescaled with respect to the refinement pass threshold $T_r^{p,m}$ given by:

$T_r^{p,m} = \max(T_{\gamma,1}^{p,m}, T_{\beta,3}^{p,m})$.

In order to improve the compression results, the output of the MD-QT coder (significance symbols, quantizer index symbols, signs symbols) are further entropy coded with an adaptive arithmetic coder [10] that uses four different probability models. One model is used to encode the quadrant significance symbols. Another model is used for the sign symbol encoding. Finally, another two models are utilized to entropy code the symbols generated by the index allocation operators $\alpha(w(\mathbf{l}))$ and $\beta(w(\mathbf{l}))$ respectively. Since the MD-QT output for the partition cells that are not divided is represented by only one symbol $S_{\gamma,1}$, it is completely redundant to further encode these symbols.

4. EXPERIMENTAL RESULTS

To perform the comparison between the EMDSQ and MDUSQ [4], both quantizers are applied on a memoryless Laplacian source of random generated numbers with zero mean and $\sigma = 60.34$, simulating a wavelet subband. Fig. 3 shows that comparable results are obtained for the side channel(s) and that the EMDSQ outperforms MDUSQ for the central channel. Similar experimental results were obtained varying the standard deviation within the range $12 < \sigma < 90$.

Similar to EMDSQ, the MDUSQ has been integrated in the MD-QT coding scheme, resulting into a common entropy-coding system for both types of quantizers. The results shown in Fig. 4 and Fig. 6 obtained on the Lena and Goldhill images respectively, reveal that on the central channel the EMDSQ outperforms MDUSQ with 0.52-1.08 dB. Similarly, the results obtained on a common image data set given in Table 5

show that in comparison to MDUSQ, the MDC system employing the EMDSQ provides constantly better rate-distortion performances on the central channel for all the rates.

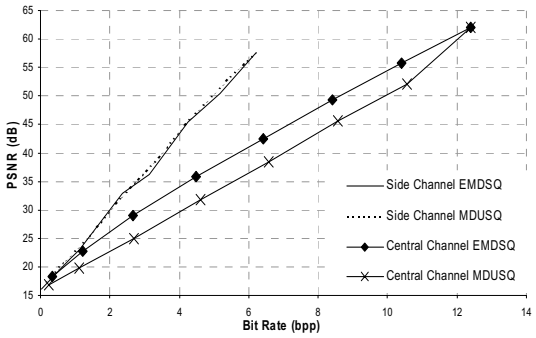

Fig. 3. Comparative side and central rate-distortion performance between EMDSQ and MDUSQ. The quantizers are applied on a 256x256 matrix of Laplacian random generated numbers with zero mean and $\sigma = 60.34$.

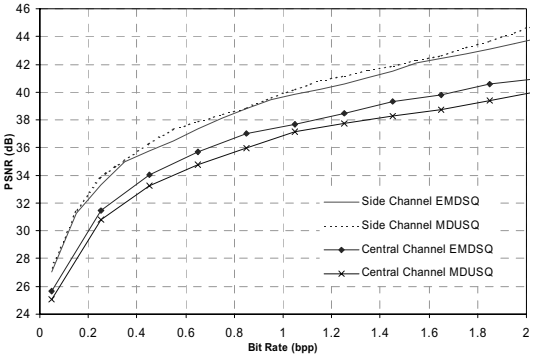

Fig. 4. Comparative side and central rate-distortion performance obtained on Lena 512x512 with the MD-QT codec employing EMDSQ and MDUSQ respectively.

Image	Quant.	0.125	0.25	0.5	1	2	4
Barbara	EMDSQ	23.90	25.72	28.52	32.56	37.75	44.52
	MDUSQ	23.63	24.87	28.20	32.16	37.15	42.85
Bird	EMDSQ	30.98	34.31	37.94	41.46	44.82	50.04
	MDUSQ	30.15	33.40	37.15	40.66	43.78	48.88
Cameraman	EMDSQ	23.32	25.26	28.08	31.78	37.06	44.43
	MDUSQ	22.59	24.80	27.50	30.87	36.21	43.08
Peppers	EMDSQ	27.80	30.79	33.53	36.04	38.60	44.11
	MDUSQ	27.28	30.14	32.97	35.45	37.78	42.21
Zelda	EMDSQ	32.64	35.22	37.75	39.84	42.41	47.71
	MDUSQ	32.11	34.74	37.13	39.23	41.73	46.63
average mean diff.		0.58	0.67	0.58	0.66	0.80	1.43

Table 5. Performance (PSNR) of the central reconstruction of MD-QT coding based on EMDSQ and MDUSQ for bit-rates ranging from 0.125 to 4 bpp.

5. CONCLUSIONS

The paper presents a new type of wavelet based MDC systems, called here MD-QT, that relies on embedded multiple description scalar quantizers and on the quadtree coding of the significance maps. The EMDSQ fulfill the requirement of a high redundancy level and enable the MD-QT codec to perform progressive image transmission over unreliable channels. For the targeted high redundancy level, the MD-QT system based on EMDSQ outperform the MD-QT system based on MDUSQ for the central channel. Thus, for an erosion channel model characterized by burst errors, coding techniques based on EMDSQ provide consistently better rate-distortion performance. Also, for the particular case when an entire channel is lost, the experiments show comparable results for the side channels. Moreover, the generalization of the codec for an arbitrary number of channels leads to the possibility of designing realistic codecs for practical multi-channel communication systems.

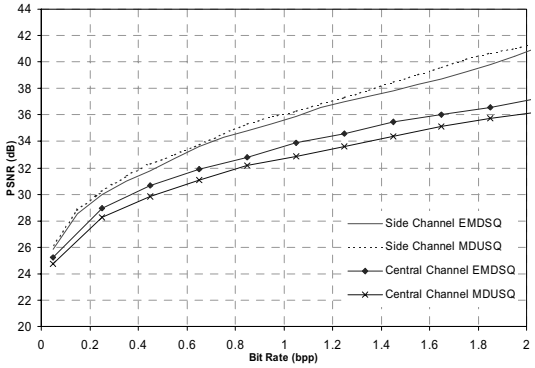

Fig. 6. Comparative side and central rate-distortion performance obtained on Goldhill 512x512 with the MD-QT codec employing EMDSQ and MDUSQ respectively.

6. REFERENCES

[1] L. Ozarow, "On a source coding problem with two channels and tree receivers," *Bell Syst. Tech. J.*, vol. 59, no., pp. 1909-1921, 1980.

[2] V. A. Vaishampayan, "Design of multiple description scalar quantizers," *IEEE Trans. Inform. Theory*, vol. 39, no. 3, pp. 821 - 834, 1993.

[3] V. A. Vaishampayan and J. Domaszewicz, "Design of entropy-constrained multiple description scalar quantizers," *IEEE Trans. Inform. Theory*, vol. 40, no. 1, pp. 245-250, 1994.

[4] T. Guionnet, C. Guillemot, and S. Pateux, "Embedded multiple description coding for progressive image transmission over unreliable channels," *Proc. IEEE Int. Conf. Image Proc.*, ICIP'01, pp. 94 - 97, 2001.

[5] W. Jiang and A. Ortega, "Multiple description coding via polyphase transform and selective quantization," *Proc. SPIE Int. Conf. Visual Comm. Image Proc.* VCIP'99, San Jose, USA, pp. 998-1008, 1999.

[6] A. Gavrilescu, A. Munteanu, P. Schelkens, and J. Cornelis, "Embedded Multiple Description Scalar Quantizer for Progressive Image Transmission," *Proc. IEEE Int. Conf. Acoustics, Speech and Signal Proc.,* ICASSP'03, Hong Kong, vol. 5, pp. 736-739, 2003.

[7] A. Gavrilescu, A. Munteanu, P. Schelkens, and J. Cornelis, "Embedded multiple description scalar quantizers," *IEE Electronics Letters*, vol. 39, no. 13, pp. 979-980, 2003.

[8] A. Munteanu, J. Cornelis, G. Van der Auwera, and P. Cristea, "Wavelet-based lossless compression scheme with progressive transmission capability," *Int. J. Imaging Systems and Tech.*, vol. 10, no. 1, pp. 76-85, 1999.

[9] D. Taubman and M. W. Marcelin, *JPEG2000: Image Compression Fundamentals, Standards, and Practice.* Norwell, Massachusetts: Kluwer Academic Publishers, 2002.

[10] I. H. Witten, R. M. Neal, and J. G. Cleary, "Arithmetic coding for data compression," *Communications of the ACM*, vol. 30, no. 5, pp. 520-540, 1987.